

# DC-DC Bidirectional Buck-Boost Topology: Design and Simulation

May 11, 2025



Zbigniew Michalak

# Contents

<b>1</b>	<b>Introduction</b>	<b>3</b>
<b>2</b>	<b>Results</b>	<b>4</b>
2.1	Steady-State Operation . . . . .	4
2.2	Bi-Directional Energy Transfer . . . . .	7
2.3	Diode and Transistor Waveforms . . . . .	8
<b>3</b>	<b>Component Selection</b>	<b>10</b>
3.1	Power Semiconductor Selection . . . . .	10
<b>4</b>	<b>Conclusion</b>	<b>10</b>

# 1 Introduction

This report presents the design and simulation of a bidirectional DC-DC converter for energy transfer between two DC voltage sources, 1. The system is designed to interface a 500V source with a 750V source, with a nominal power rating of 3.5kW and a PWM controller 2. Bidirectional power flow capability is essential for applications such as energy storage systems, electric vehicle charging stations, and renewable energy interfaces.

The converter topology was selected to efficiently handle the voltage conversion ratio while allowing power flow in both directions. The design process focused on determining appropriate component values, especially the inductor sizing, to meet specified ripple requirements. All simulations were performed using PLECS.

The following sections detail the design calculations, component selection methodology, and analysis of the simulation results demonstrating the converter's performance in various operating conditions.

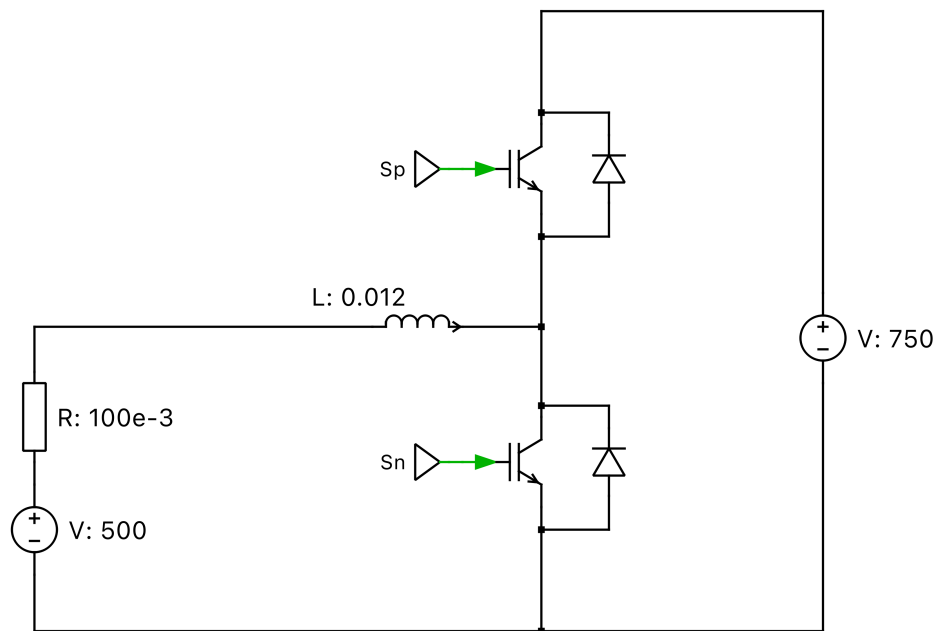


Figure 1: Circuit schematic.

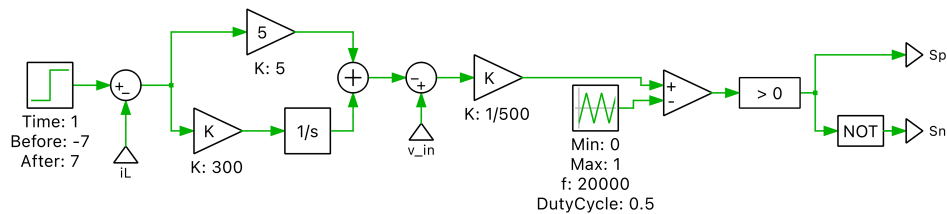


Figure 2: PWM controller schematic.

## 2 Results

The following figures present the simulation results for the bi-directional DC-DC converter operating between a 500V source and a 750V source, designed for a nominal power of 3.5kW and a switching frequency of 20kHz. The inductor value is  $L=0.012H$ . It should be noted that the actual power in the simulation might differ slightly from the nominal value due to the addition of a 100mΩ resistor placed in series with the input DC source. This resistor was necessary to improve circuit stability and dampen parasitic oscillations that can occur in ideal switching simulations.

### 2.1 Steady-State Operation

Figure 3 shows the inductor current ( $I_L$ ) during converter steady-state operation. The average inductor current ( $I_{L,avg}$ ) can be calculated as:

$$I_{L,avg} = \frac{P_{nom}}{V_{in}} = \frac{3500W}{500V} = 7A \quad (1)$$

The inductor current ripple ( $\Delta i_L$ ) can be observed around this average value, meeting the design requirement of less than 10% (0.7A for the 7A average current). This was achieved by calculating the correct inductor value.

According to the simulation, the voltage across the inductor alternates between 500V and -250V. This can be explained as follows:

- When the upper switch is ON and lower switch is OFF:  $V_L = V_{in} - V_{out} = 500V - 750V = -250V$
- When the upper switch is OFF and lower switch is ON:  $V_L = V_{in} = 500V$

For a boost mode operation with duty cycle  $D$  (fraction of time when the lower switch is ON), we can derive the inductor equation from the basic inductor voltage-current relationship:

$$L = \frac{V_L \cdot \Delta t}{\Delta i_L} = \frac{V_{in} \cdot (D/f_s)}{\Delta i_L} = \frac{V_{in} \cdot D}{f_s \cdot \Delta i_L} \quad (2)$$

This equation represents the relationship between inductor size and current ripple. It means that:

- $V_L$  is the voltage across the inductor ( $V_{in}$  during ON time)
- $\Delta t$  is the duration of the ON time ( $D/f_s$ )
- $V_{in}$  is the input voltage applied across the inductor during the ON time
- $D$  is the duty cycle (fraction of the switching period when voltage  $V_{in}$  is applied)
- $f_s$  is the switching frequency, determining how often the cycle repeats
- $\Delta i_L$  is the allowed current ripple

For our bidirectional DC-DC converter with boost operation (500V to 750V):

$$V_{out} = \frac{V_{in}}{1-D} \implies D = 1 - \frac{V_{in}}{V_{out}} = 1 - \frac{500V}{750V} = 1 - \frac{2}{3} = \frac{1}{3} \quad (3)$$

$$\Delta i_L = 10\% \cdot I_{L,avg} = 0.1 \cdot 7A = 0.7A \quad (4)$$

Therefore:

$$L = \frac{V_{in} \cdot D}{f_s \cdot \Delta i_L} = \frac{500V \cdot \frac{1}{3}}{20kHz \cdot 0.7A} = \frac{166.7V}{14kA} = 11.9mH \approx 12mH \quad (5)$$

This confirms that the design value of  $L=12\text{mH}$  is appropriate to keep the current ripple below 10% of the average current.

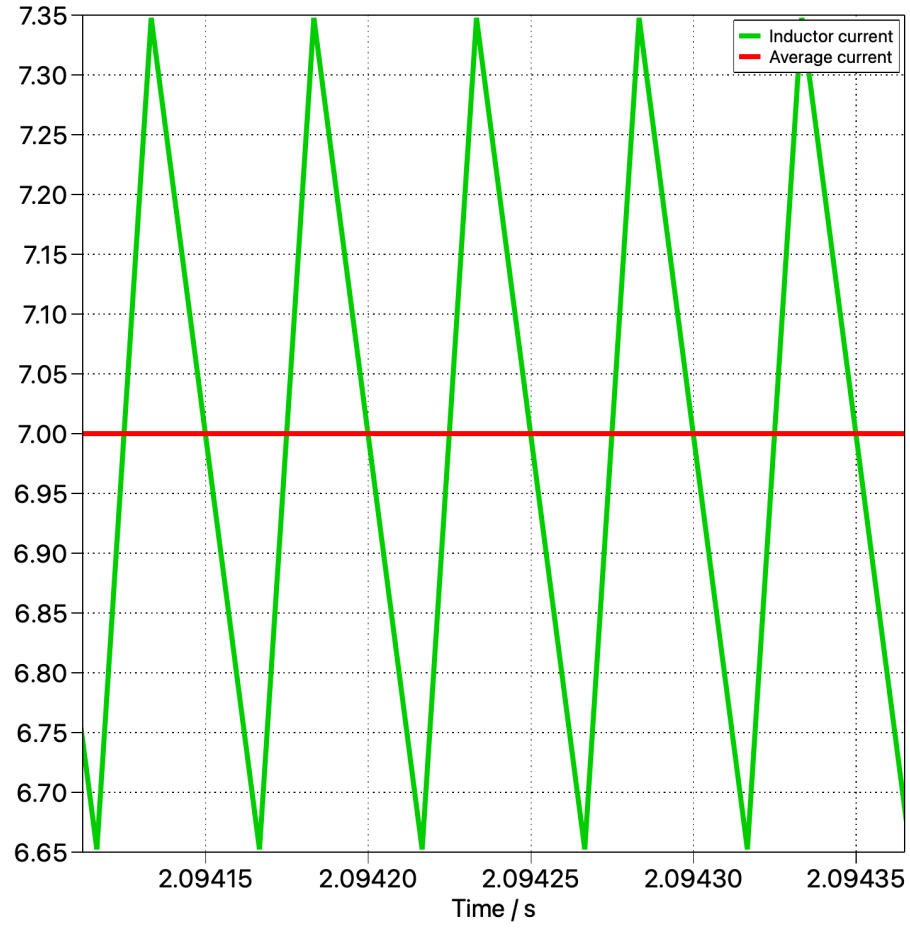


Figure 3: Inductor current ( $I_L[A]$ ) showing average value and ripple.

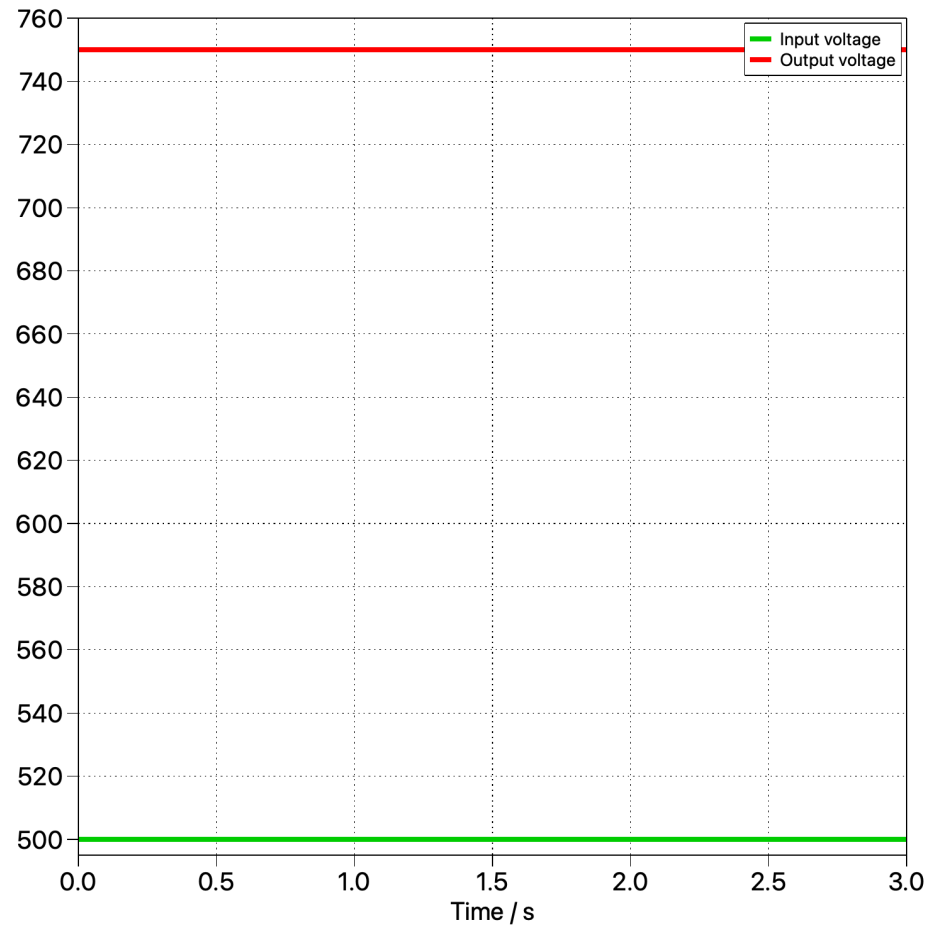


Figure 4: Input and Output Voltages ( $V_{in}, V_{out}$ ).

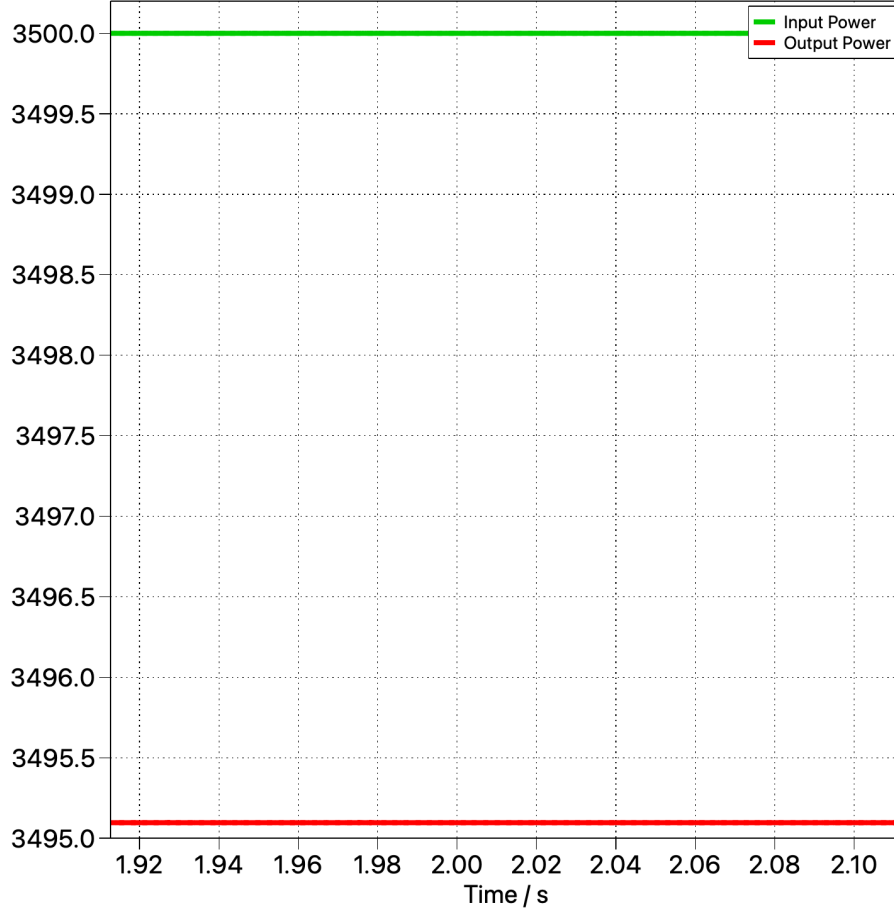


Figure 5: Instantaneous Power [W].

**Note on Power Discrepancy:** The slight difference between the nominal power and the simulated power values observed in Figure 5 is due to the presence of a  $100\text{ m}\Omega$  resistor placed in series with the input voltage source. This resistor introduces a small voltage drop and dissipates part of the total power as heat, leading to a slightly reduced power delivered to the main converter circuit.

## 2.2 Bi-Directional Energy Transfer

Figure 6 demonstrates the converter's capability for bi-directional power flow. The plot shows the inductor current ( $I_L$ ) transitioning between positive ( $I_L > 0$ , power flow from 500V to 750V) and negative ( $I_L < 0$ , power flow from 750V to 500V) values over a longer time scale than the steady-state plots. This transition is achieved by changing the control reference from  $-7\text{ A}$  to  $7\text{ A}$  at time of 1s.

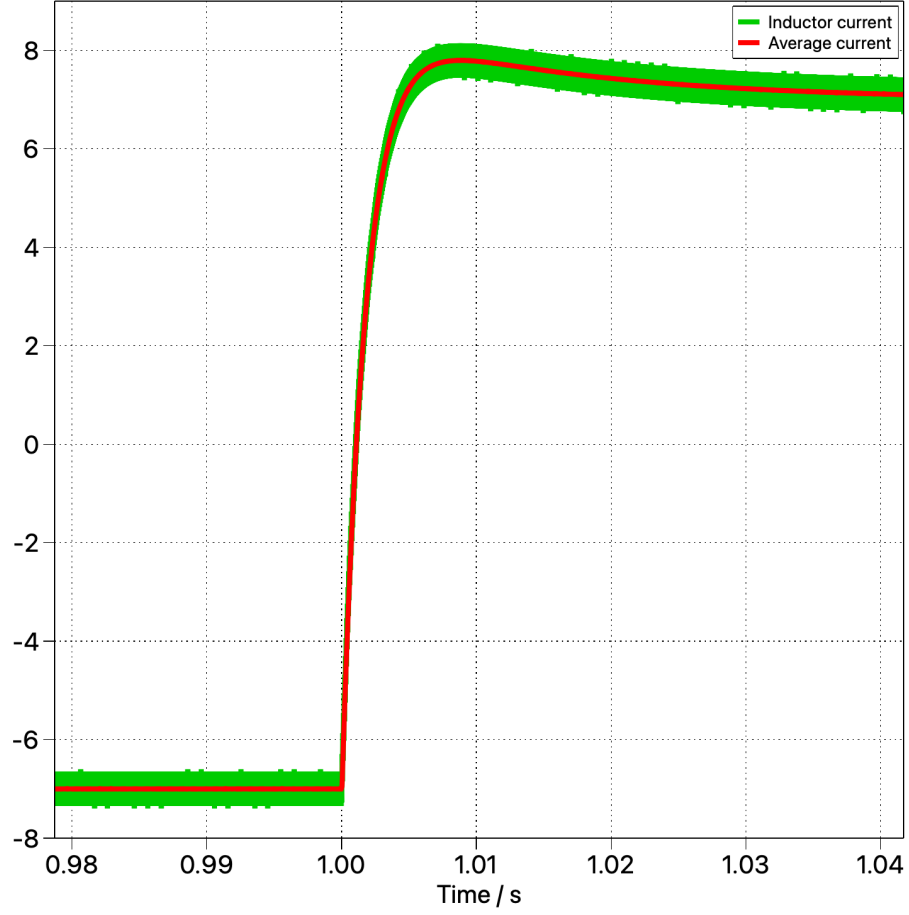


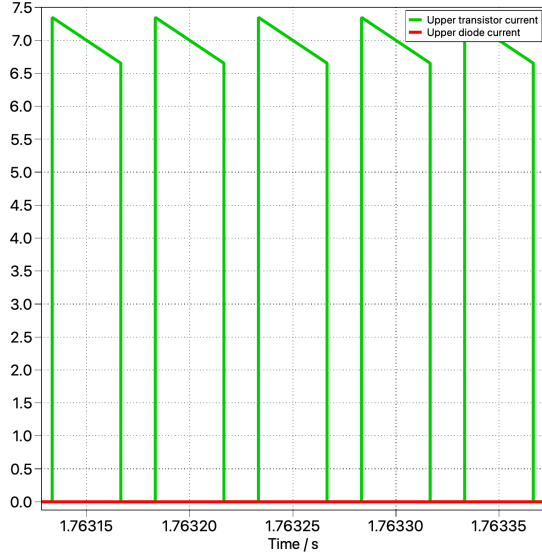
Figure 6: Inductor current ( $I_L$ ) showing transition between positive and negative values at time of 1s, indicating bi-directional energy transfer.

### 2.3 Diode and Transistor Waveforms

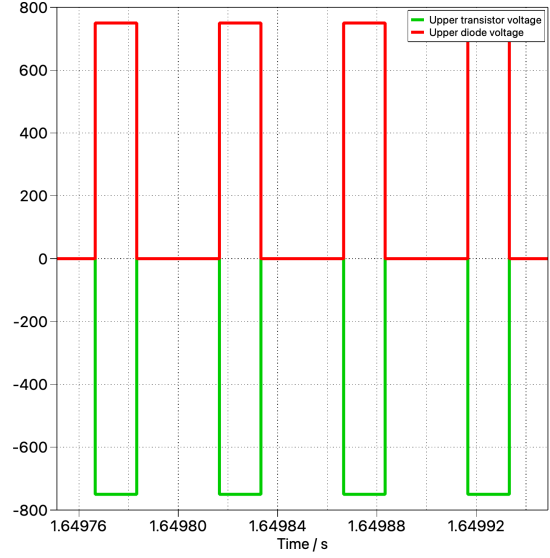
Figures 7 and 8 show the detailed voltage and current waveforms for the semiconductor devices during one switching period in steady-state operation.

Figure 7 displays the currents and voltages for the upper diode and transistor. Subfigure 7a shows the current waveforms ( $i_{D,u}$ ,  $i_{T,u}$ ), and Subfigure 7b shows the corresponding voltage waveforms ( $v_{D,u}$ ,  $v_{T,u}$ ).





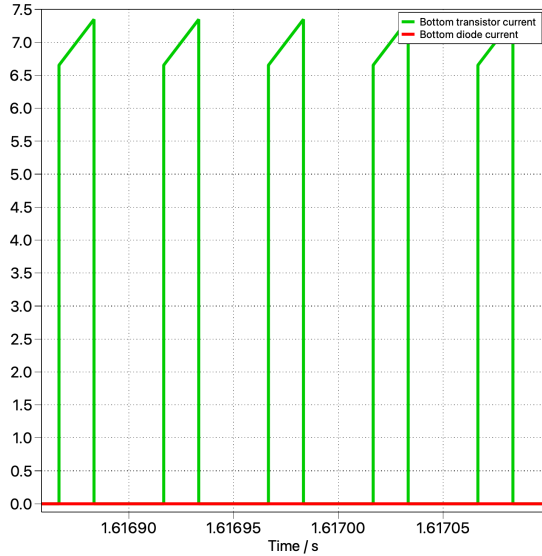
(a) Current waveforms ( $i_{D,u}, i_{T,u}$ )



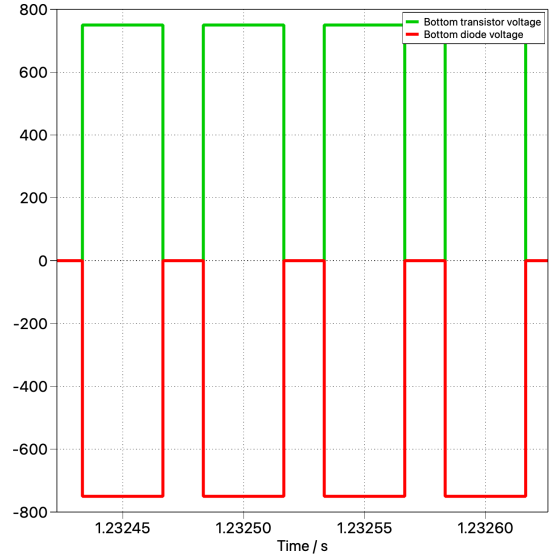
(b) Voltage waveforms ( $v_{D,u}, v_{T,u}$ )

Figure 7: Waveforms for the upper diode and transistor.

Figure 8 displays the currents and voltages for the bottom diode and transistor. Subfigure 8a shows the current waveforms ( $i_{D,b}, i_{T,b}$ ), and Subfigure 8b shows the corresponding voltage waveforms ( $v_{D,b}, v_{T,b}$ ). These plots complement Figure 7 by showing the behavior of the complementary devices in the converter leg.



(a) Current waveforms ( $i_{D,b}, i_{T,b}$ )



(b) Voltage waveforms ( $v_{D,b}, v_{T,b}$ )

Figure 8: Waveforms for the bottom diode and transistor.

## 3 Component Selection

### 3.1 Power Semiconductor Selection

For this bidirectional DC-DC converter design, the Wolfspeed C3M0065090J Silicon Carbide Power MOSFET was selected as the primary switching device. This component offers several key advantages that make it ideal for this application:

**Maximum Ratings** ( $T_c = 25^\circ\text{C}$  unless otherwise specified)

Symbol	Parameter	Value	Unit	Test Conditions	Note
$V_{DSmax}$	Drain - Source Voltage	900	V	$V_{GS} = 0\text{ V}, I_D = 100\text{ }\mu\text{A}$	
$V_{GSmax}$	Gate - Source Voltage (dynamic)	-8/+19	V	AC ( $f > 1\text{ Hz}$ )	Note. 1
$V_{GSop}$	Gate - Source Voltage (static)	-4/+15	V	Static	Note. 2
$I_D$	Continuous Drain Current	35	A	$V_{GS} = 15\text{ V}, T_C = 25^\circ\text{C}$	Fig. 19
		22		$V_{GS} = 15\text{ V}, T_C = 100^\circ\text{C}$	
$I_{D(pulse)}$	Pulsed Drain Current	90	A	Pulse width $t_p$ limited by $T_{jmax}$	Fig. 22
$E_{AS}$	Avalanche energy, Single pulse	110	mJ	$I_D = 22\text{ A}, V_{DS} = 50\text{ V}$	
$P_D$	Power Dissipation	113	W	$T_C = 25^\circ\text{C}, T_J = 150^\circ\text{C}$	Fig. 20
$T_J, T_{stg}$	Operating Junction and Storage Temperature	-55 to +150	$^\circ\text{C}$		
$T_L$	Solder Temperature	260	$^\circ\text{C}$	1.6mm (0.063") from case for 10s	

Note (1): When using MOSFET Body Diode  $V_{GSmax} = -4\text{V}/+19\text{V}$

Note (2): MOSFET can also safely operate at 0/+15 V

Figure 9: Wolfspeed C3M0065090J Silicon Carbide Power MOSFET Specification

The C3M0065090J MOSFET is particularly well-suited for this bidirectional DC-DC converter application for the following reasons:

- **High Voltage Rating:** With a  $V_{DS}$  rating of 900V, this MOSFET provides significant voltage headroom above our maximum system voltage of 750V, ensuring safe operation even during transient conditions.
- **High Current Capacity:** The continuous drain current rating of 35A exceeds our nominal current requirements (7A), allowing for power scaling and transient handling capability.
- **Silicon Carbide Technology:** Compared to traditional silicon MOSFETs, SiC technology offers lower on-state resistance, reduced switching losses, and higher temperature operation capability, resulting in improved efficiency for our high-power bidirectional converter.
- **Fast Switching Capability:** The device features low gate charge and output capacitance, enabling efficient operation at our 20kHz switching frequency while minimizing switching losses.

## 4 Conclusion

The designed bidirectional DC-DC converter successfully demonstrates the ability to facilitate power flow between a 500V source and a 750V source with a nominal power rating of 3.5kW. Through careful component selection and design calculations, the converter achieves the specified performance requirements:

- The inductor value of 12mH limits the current ripple to less than 10% of the average current (0.7A for a 7A average), as confirmed by both theoretical calculations and simulation results.

- The converter effectively operates in both boost mode (500V to 750V) and buck mode (750V to 500V), demonstrating true bidirectional energy transfer capability.
- The semiconductor devices (diodes and transistors) show appropriate switching behavior with voltage and current levels within expected ranges based on the design specifications.
- The selected Wolfspeed C3M0065090J Silicon Carbide Power MOSFET provides sufficient voltage (900V) and current (35A) ratings for the application, with additional benefits of SiC technology including lower switching losses and higher temperature capability.

The waveforms clearly illustrate the operation principles of the converter in different modes and provide valuable insights into the dynamic behavior of currents and voltages throughout the circuit. This bidirectional converter design could be effectively applied in various applications requiring flexible energy management between DC systems with different voltage levels, such as battery storage integration with DC microgrids or electric vehicle charging infrastructure.